THE JOURNAL OF BIOLOGICAL CHEMISTRY
Vol. 272, No. 18, Issue of May 2, pp. 11850–11855, 1997

Printed in U.S.A.

Uncoupled Phosphorylation and Activation in Bacterial Chemotaxis

THE 2.3 Å STRUCTURE OF AN ASPARTATE TO LYSINE MUTANT AT POSITION 13 OF CheY*

(Received for publication, December 18, 1996)

Meiying Jiang‡§, Robert B. Bourret¶‖, Melvin I. Simon¶, and Karl Volz‡**

From the ‡Department of Microbiology and Immunology, University of Illinois, Chicago, Illinois 60612 and the ¶Division of Biology, California Institute of Technology, Pasadena, California 91125

An aspartate to lysine mutation at position 13 of the chemotaxis regulatory protein CheY causes a constitutive tumbly phenotype when expressed at high copy number *in vivo* even though the mutant protein is not phosphorylatable. These properties suggest that the D13K mutant adopts the active, signaling conformation of CheY independent of phosphorylation, so knowledge of its structure could explain the activation mechanism of CheY. The x-ray crystallographic structure of the CheY D13K mutant has been solved and refined at 2.3 Å resolution to an *R*-factor of 14.3%. The mutant molecule shows no significant differences in backbone conformation when compared with the wild-type, Mg^{2+}-free structure, but there are localized changes within the active site. The side chain of lysine 13 blocks access to the active site, whereas its ϵ-amino group has no bonding interactions with other groups in the region. Also in the active site, the bond between lysine 109 and aspartate 57 is weakened, and the solvent structure is perturbed. Although the D13K mutant has the inactive conformation in the crystalline form, rearrangements in the active site appear to weaken the overall structure of that region, potentially creating a metastable state of the molecule. If a conformational change is required for signaling by CheY D13K, then it most likely proceeds dynamically, in solution.

Cells continuously monitor various chemical and physical parameters in their surrounding environment and use this information to implement appropriate adaptive responses to changing conditions. This vital task is accomplished by a cascade of transient protein phosphorylation and dephosphorylation events arranged so that the flow of phosphoryl groups reflects environmental conditions. One ubiquitous class of signal transduction networks is the "two-component" regulatory systems that control diverse processes such as behavior, development, physiology, and virulence in bacteria, as well as adaptive processes in eukaryotes (for reviews, see Refs. 1–4). The first component is a histidine protein kinase, which autophosphorylates using ATP as the phosphodonor. The second component is a response regulator protein, which transfers the phosphoryl group from the histidine protein kinase to itself. Response regulators are also capable of autophosphorylation using small molecule phosphodonors such as acetyl phosphate (5, 6). Phosphorylation alters the activity of the response regulator, thereby generating a response (*e.g.* change in gene expression) to the environmental stimulus.

Our goal is to understand in atomic detail the effects of phosphorylation on response regulator structure and function. The best characterized response regulator is the bacterial chemotaxis protein CheY, which has been the subject of extensive genetic, biochemical, and biophysical analyses. Phosphorylated CheY (CheY-P)[1] causes flagellar rotation to change from the default counterclockwise direction to clockwise (7–10). The coordination of changes in swimming behavior with the temporal changes in chemical concentrations experienced by cells swimming in chemical gradients results in chemotaxis (11, 12).

The three-dimensional structure of CheY has been solved by both x-ray crystallography (13–16) and multidimensional NMR (17–19). Response regulator active sites are formed from five highly conserved residues of the response regulator superfamily (20). In CheY, these are Asp^{12} and Asp^{13}, involved in binding a Mg^{2+} ion essential for the phosphorylation and dephosphorylation reactions (15, 16, 21); Asp^{57}, the site of phosphorylation (22); Thr^{87}, implicated in the postphosphorylation signaling events (23); and Lys^{109}, also required for postphosphorylation steps in the signaling pathway (24). The structure of CheY-P has not yet been determined due to the fact that the phosphoryl group has a half-life of only a few seconds on CheY (8, 9).

We adopted a mutational approach to determine the active conformation of CheY. Phosphorylation is not the only route to response regulator activation. Mutations that result in constitutive activity have been isolated for many response regulators. In the case of CheY, replacement of Asp^{13} with lysine (the D13K mutant) results in clockwise flagellar rotation (25, 26). Genetic evidence that the CheY D13K protein is activated in the absence of phosphorylation implies that the phosphoryl group does not play a direct role in the mechanism of CheY signal transduction, such as phosphotransfer to a downstream protein, or direct binding (25, 26). These results, plus biochemical evidence that CheY activation does not involve a change to a multimeric state (25, 27), lead to the conclusion that the indirect role of phosphorylation is to generate a conformational change that allows CheY to interact productively with the flagellar switch. NMR data show that CheY undergoes a conformational change upon phosphorylation (28, 29). Presumably, this conformational change is mimicked by constitutively

* This work was supported by National Institutes of Health Grants GM39919 and GM47522 (to K. V.) and AI19296 (to M. I. S.) and by a National Research Service Award Fellowship AI07798 (to R. B. B.). The costs of publication of this article were defrayed in part by the payment of page charges. This article must therefore be hereby marked "*advertisement*" in accordance with 18 U.S.C. Section 1734 solely to indicate this fact.

The atomic coordinates and structure factors (code pdb1ehc.ent and r1ehc.ss) have been deposited in the Protein Data Bank, Brookhaven National Laboratory, Upton, NY.

§ Present address: Dept. of Public Policy, University of Chicago Chicago, Il 60637.

‖ Present address: Dept. of Microbiology and Immunology, University of North Carolina, Chapel Hill, NC 27599-7290.

** To whom correspondence should be addressed. Tel.: 312-996-2314; 312-996-6415; Fax: karl@e002.mim.uic.edu.

[1] The abbreviation used is: CheY-P, phosphorylated CheY.

TABLE I
Statistics for data and final refinement of Escherichia coli CheY mutant D13K

Resolution limits	No. reflections predicted	Complete	$\geq 2\sigma_F$	Refinement R-value[a]
Å		%		%
$\infty \rightarrow 10.00$	86	96.5	–[b]	–
$10.00 \rightarrow 4.32$	816	100.0	96.9	14.8
$4.32 \rightarrow 3.43$	834	100.0	95.9	11.2
$3.43 \rightarrow 3.00$	826	99.9	92.9	12.5
$3.00 \rightarrow 2.72$	835	97.0	86.5	14.9
$2.72 \rightarrow 2.52$	846	94.4	75.8	17.1
$2.52 \rightarrow 2.37$	822	85.2	64.1	20.6
$2.37 \rightarrow 2.26$	755	31.9	24.4	20.2
$10.00 \rightarrow 2.26$	5820	87.8	76.2	14.3

[a] $R = \frac{\Sigma|F_{obs} - F_{calc}|}{\Sigma|F_{obs}|} \times 100$
[b] Data intentionally omitted.

TABLE II
Refinement restraints and root mean square deviations from ideal of the E. coli CheY mutant D13K using 4432 reflections from 10 to 2.26 Å

Parameter	Target σ	Final value
Distance restraints (Å)		
Bond distance	0.020	0.016
Angle distance	0.040	0.051
Planar distance	0.050	0.057
Plane restraint (Å)	0.020	0.010
Chiral-center restraint (Å^3)	0.150	0.153
Non-bonded contact restraints (Å)		
Single torsion contact	0.500	0.201
Multiple torsion contact	0.500	0.238
Possible hydrogen bond	0.500	0.287
Conformational torsion angle restraint (Å)		
Planar (ω, 0°, 180°)	3.0	1.8
Staggered (±60°, 180°)	15.0	20.5
Orthonormal (±90°)	20.0	17.6
Isotropic thermal factor restraints (Å^2)		
Main-chain bond	1.000	0.823
Main-chain angle	1.500	1.431
Side-chain bond	1.000	0.916
Side-chain angle	1.500	1.614
X-ray	$0.7*\langle\|F_o - F_c\|\rangle$	14.30%

active mutants such as CheY D13K. The two routes of activation (phosphorylation *versus* the D13K mutation) are thought to have the same mechanistic features because Lys^{109} is essential for both (24, 26). We therefore solved the x-ray crystal structure of the D13K CheY mutant to find the activated conformation of CheY.

MATERIALS AND METHODS

Protein Purification—CheY D13K was purified as described previously (30), except on a larger scale. A 100 liter culture of KO641recA/pRBB40.13DK (25) was grown in LB + 100 μg/ml ampicillin in a fermentor at 37 °C. Expression of CheY D13K was induced at a cell turbidity of A_{595} = 1 by addition of 3β-indoleacrylic acid to 100 μg/ml final concentration. Cells were harvested after 2 h. Approximately 11 liters of cell paste were lysed by sonication and clarified by centrifugation. TEDG buffer (50 mM Tris-HCl, pH 7.5, 1 mM EDTA, 2 mM dithiothreitol, and 10% v/v glycerol) was used throughout the purification procedure. The cell lysate was loaded onto a 2.5 × 10 cm (50 ml) Affi-Gel Blue column, washed, and eluted with a 0–0.6 M NaCl gradient. Two passes were required on the Blue column to separate the D13K from the flow-through. The fractions containing the D13K were pooled, desalted by dilution, and concentrated in a stirred cell ultrafiltration unit with a PM10 membrane (Amicon, Inc.). The concentrated D13K was loaded on a 2.5 × 10 cm (50 ml) DEAE-Sepharose CL-6B column and immediately eluted with 0.025 M NaCl. CheY D13K was found to bind to DEAE less tightly than wild-type CheY, presumably due to the +2 charge change resulting from the mutation. Finally, all fractions containing D13K were pooled, concentrated with Centricon-10 concentrators (Amicon, Inc.), and applied to a Superose 12 HR16/50 fast protein liquid chromatography gel filtration column (Pharmacia Biotech Inc.). Fractions containing pure D13K were stored at −20 °C.

Approximately half of the CheY D13K (molecular mass = 14 kDa) passed through the PM10 filter (molecular mass cutoff 10 kDa) at the pre-DEAE step. Passage through the filter resulted in substantial purification, so this material was retrieved, concentrated in a stirred cell ultrafiltration unit with a YM5 membrane (Amicon, Inc.), and chromatographed separately on the DEAE column. The overall yield from both halves of the purification process was 28 mg of D13K.

Protein Crystallization—The purified protein was precipitated in a solution of 3.2 M ammonium sulfate, centrifuged, redissolved in a minimal volume of 80 mM ammonium sulfate, 50 mM Tris-HCl, pH 8.3, and brought to a final concentration of 15 mg/ml. The protein was then loaded into 20-μl microdialysis chambers, each sealed with dialysis membrane. Ammonium sulfate was the precipitant used in the crystallization trials. The critical ammonium sulfate concentration for nucleation and crystallization was found to be 2.2 M. The pulsed-diffusion method (31) was used as described previously (32) for optimization of crystal size and quality, where graduated up- and down-pulses were explored over the range of 0.1–2.5 M ammonium sulfate. The crystal used for data collection grew to dimensions of 0.90 × 0.08 × 0.08 mm.

Mg^{2+} is required in the phosphorylation and dephosphorylation reactions of wild-type CheY (5, 21, 33). However, Mg^{2+} binding to CheY D13K is not detectable by either resonance shifts in ^{19}F NMR spectra of 4-fluorophenylalanine-labeled protein or by quenching of Trp^{58} fluorescence (28, 34). Lack of metal ion binding to the mutant protein is consistent with the observation that in wild-type CheY, Asp^{13} is directly involved in coordination of the Mg^{2+} ion (15, 16). Furthermore, D13K is phosphorylated only very slowly in the presence of the histidine protein kinase CheA and ATP (26, 27), and apparently not at all in the presence of acetyl phosphate (34). Thus, crystallization of CheY D13K in the absence of both Mg^{2+} and phosphate is biologically relevant.

Crystallographic Data Collection and Processing—Crystals of the CheY D13K mutant were indistinguishable from those of wild-type CheY, belonging to the orthorhombic space group $P2_12_12_1$, with unit cell dimensions of a = 45.9 Å, b = 47.0 Å, and c = 54.0 Å. Diffraction data were collected from one crystal at the area detector facility at Argonne National Laboratory. The crystal was exposed for a total of ~42 h in graphite monochromatized Cu K_α radiation from a rotating anode x-ray generator (50 kV, 100 mA) passing through a 0.3-mm collimator. Data were recorded at a crystal to detector distance of 100 mm on a Siemens multiwire area detector, with a swing angle of 15° in 2θ for a theoretical upper resolution limit of 2.26 Å. Data processing and reduction was done using the XENGEN program package (35). The cell parameters determined by XENGEN deviated from wild-type by only 0.26%. The final data set included a total of 12,828 observations of 5,820 unique reflections ranging from infinity to 2.26 Å. The unweighted absolute R-factor on intensities for merging all reflections was 6.02%. Statistics for the final data set used in the structural solution are given in Table I.

Phasing and Structural Refinement—Because the CheY D13K crystals were isomorphous with those of wild-type apoCheY, phasing of the D13K structure was initiated with a phase calculation using the wild-type structure with all solvent molecules excluded, and residue 13 was modeled as an alanine. Refinement of atomic positions was done using the restrained least squares method (36). The R-factor smoothly converged to a final value of 14.3% after a total of 110 cycles of refinement interspersed with 10 partial rebuilds. 4,432 reflections greater than 2σ in the resolution range 10–2.26 Å were used in the final refinement. The final refinement status is presented in Table II.

Calculations of electron density maps and other data processing were carried out with the XTAL software package (37) and several locally developed programs. The least squares refinement was done with the software packages PROTIN and PROFFT (36, 38). Visualization of the electron density maps and model rebuilding were done using the graphics package FRODO (39) on an Evans and Sutherland PS300 system.

RESULTS

General Description of Structural Results—The electron density maps from the final $|2F_o - F_c|\alpha_{calc}$ and $|F_o - F_c|\alpha_{calc}$ difference Fourier calculations are clear and well defined for the entire backbone of the molecule. The average thermal parameters for all protein atoms is 13.8 Å^2 (Fig. 1). The final coordinate set consists of 1108 atoms, of which 1003 are protein and 105 are solvent molecules with unit occupancies.

Clearly defined electron density for the entire lysine residue at position 13 confirms the amino acid substitution (Fig. 2). The amino group of the Lys^{13} side chain makes no interactions with other groups of the active site. Instead, the side chain is in a fairly extended conformation (χ_{1-4} = 70°, −156°, 152°, and 123°, respectively), where the ϵ-amino group has weak hydrogen bonding contacts with external solvent molecules. The non-ideal value of χ_4 is due to a close, non-bonding contact of the terminal group with the side chain of Asn^{59}. Although the lysine side chain at position 13 appears capable of assuming an alternate rotameric position (t) away from the active site with no steric restrictions, its observed position (g^-) in the structure blocks access to the active site, especially the Mg^{2+} binding region. This is consistent with the fact that the CheY D13K mutant does not bind Mg^{2+} (34) and exhibits essentially no phosphorylation ability (26, 27, 34).

Comparison of Wild-type and CheY D13K Structures—A least squares superposition of the Mg^{2+}-free, wild-type, and D13K mutant CheY structures shows a root mean square difference in positions of equivalent α-carbon atoms of just 0.21 Å and reveals only one significant difference in the position of backbone atoms, 0.71 Å for the α-carbon of Lys^{13}, the site of the mutational change (Fig. 3).

There are only two side chains that differ in position by any significant extent between the two structures, Asp^{12} and Asp^{57} (Fig. 4). In the CheY D13K structure, Asp^{12} is rotated by −50° about its χ_2 bond, where its $O_{\delta 1}$ atom establishes a hydrogen bond with the amide nitrogen of Phe^{14}. Similarly, Asp^{57} is rotated by −60° about its χ_2 bond, so the Asp^{57} $O_{\delta 2}$ atom loses its hydrogen bond with the amide nitrogen of Asn^{59}. The new position of the Asp^{57} side chain is 1.1 Å closer to the Mg^{2+} binding site, a site now unoccupied because of the occlusion by the Lys^{13} side chain. This repositioning of Asp^{57} eliminates its strong interaction with the ϵ-amino group of Lys^{109} seen in the wild-type CheY structure. The only other change in the CheY D13K mutant is the pronounced lack of order in the solvent structure of the active site. In wild-type CheY, the active site contains some of the best ordered solvent molecules, whereas in the D13K structure, the solvent is poorly ordered and with much higher temperature factors and weaker hydrogen bonding geometries (Fig. 4).

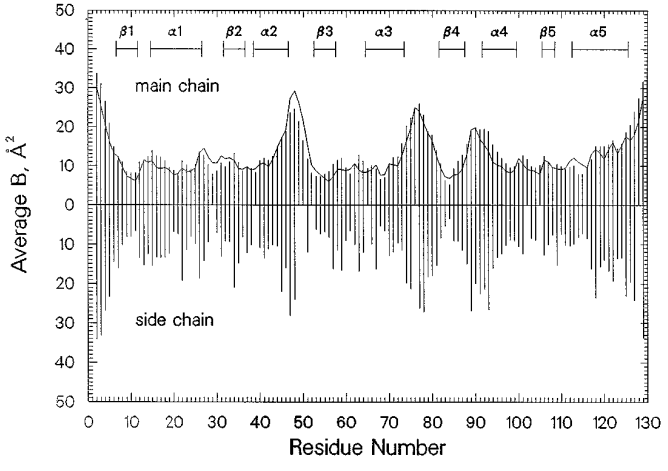

FIG. 1. **Temperature factor *versus* residue number for CheY mutant D13K.** Temperature factors for main chain and side chain groups were calculated from arithmetic averages of their respective atoms. The average main chain temperature factors for wild-type CheY are plotted as a *continuous line* for comparison. A schematic of the secondary structure elements is included.

DISCUSSION

Wild-type CheY and CheY D13K Have the Same Conformation in the Crystalline State—The presumably inactive, non-phosphorylated, wild-type CheY and the presumably activated D13K mutant CheY have backbone conformations in the crystalline state that are indistinguishable within experimental error. There are three possibilities that could account for this result. First, activation of CheY might not involve a conformational change. There is at least one example of lack of conformational changes in an enzyme following phosphorylation (40, 41), concerning the regulation of isocitrate dehydrogenase.

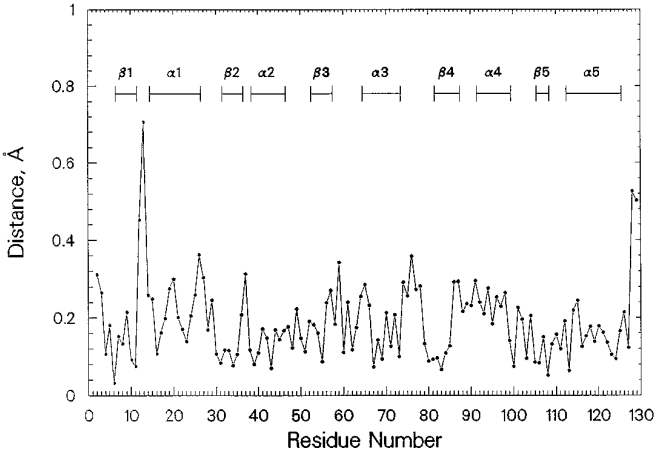

FIG. 3. ***rms* differences between α-carbon positions of D13K mutant and wild-type CheY molecules after least squares superposition.** The average *rms* difference for all α-carbon atoms is 0.21 Å.

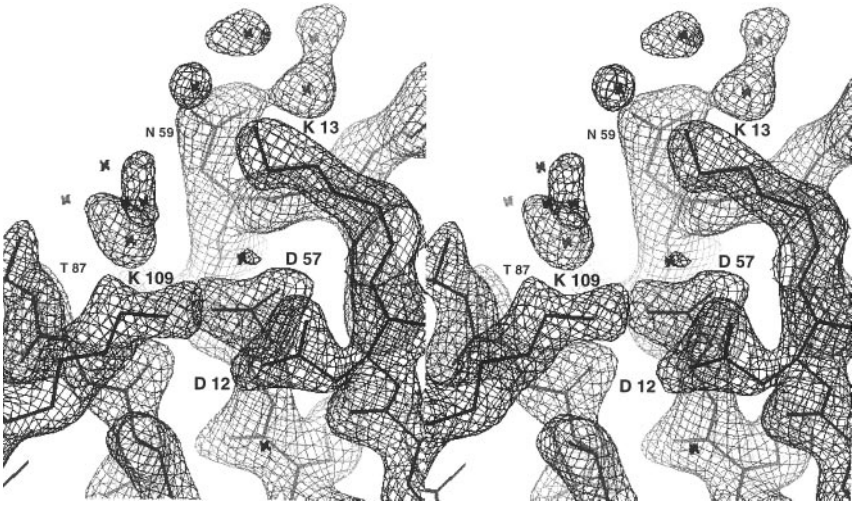

FIG. 2. **Stereo diagram of the final $|2F_o - F_c|\alpha_{calc}$ electron density map of the D13K mutation site of CheY.** The map was contoured at 1.5σ. Parts of the map, molecule, and solvent between the viewer and the active site have been removed for clarity.

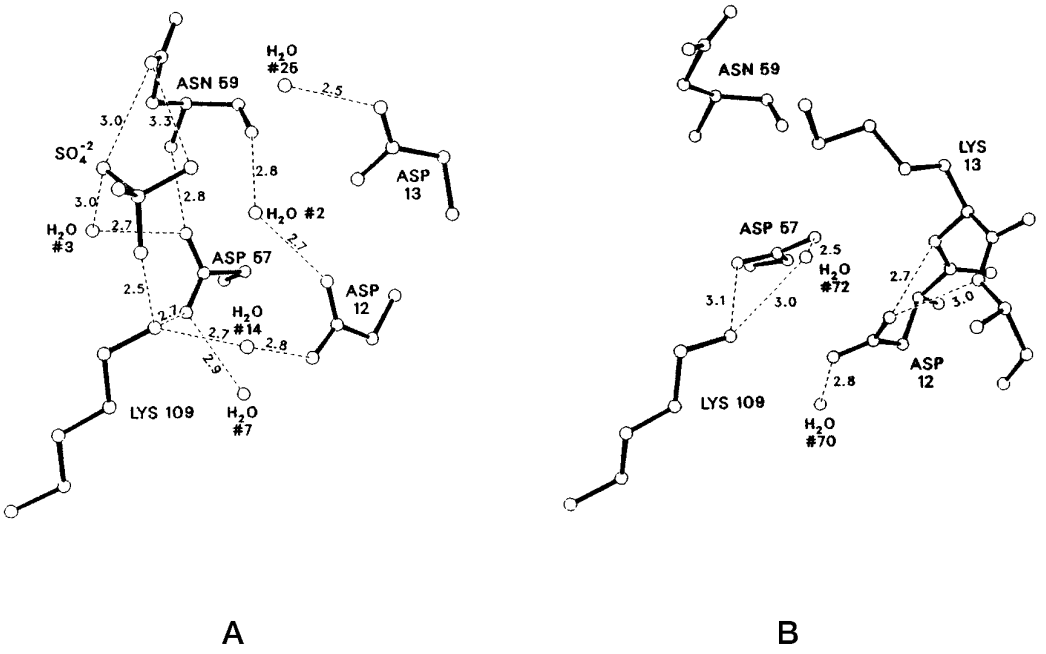

FIG. 4. **Comparison of CheY active sites.** *A*, active site of wild-type CheY at 1.7 Å resolution (14). *B*, active site of CheY D13K at 2.3 Å resolution. The orientation is approximately the same as in Fig. 2. The solvent molecules are *numbered* in order of increasing temperature factors for each structure.

However, this explanation does not apply to CheY because it is inconsistent with all previous experimental data (25, 27–29) as described in the Introduction. Second, both proteins might have crystallized in the active conformation. This is unlikely because the conformation observed in crystalline CheY D13K is the same as wild-type, apoCheY, both crystalline (13–15) and in solution (17–19), and the conformation of wild-type CheY has been shown to change upon Mg^{2+} binding (15, 16, 18, 28, 42) and phosphorylation (28, 29). Thus, these results strongly suggest the third possibility that the conformation of D13K observed here does not represent the activated state of CheY.

There are three possible explanations why the D13K CheY mutant might have crystallized in an inactive conformation. First, it might assume the active conformation only upon binding to the flagellar switch. This seems improbable, and also not readily testable. Second, in solution, D13K might truly mimic the phosphorylation-induced conformational changes that are critical for activation, but lattice forces prevent the solution-state conformational change from occurring in the crystal. This seems unlikely in view of the facts that the crystallization conditions, crystal morphology, space group, and unit cell dimensions were identical for Mg^{2+}-free, wild-type CheY and D13K. Finally, the CheY molecule may normally exist in equilibrium between the active and inactive conformations, and either phosphorylation or the D13K mutation could serve to shift a sufficient fraction of the population into the activated state to generate clockwise flagellar rotation *in vivo* (Fig. 5). With this explanation, the observed, crystalline conformation of CheY D13K would be a metastable state, the conformation of the inactive majority of the population, which could transform to the activated form in solution. This possibility is consistent with results from ^1H- and ^{15}N-NMR spectroscopy on CheY D13K, which allow for a small percent of the D13K mutant molecule to be in an alternate conformation, rapidly interconverting with its resting state.[2]

Comparison of Wild-type and CheY D13K Activities—CheY binds specifically to three different proteins: CheA, which donates the phosphoryl group to CheY (43–46); CheZ, which stimulates dephosphorylation of CheY-P (43, 47–49); and FliM, the recipient of the activating signal of CheY, located in the flagellar switch complex (34, 50). Phosphorylation of wild-type CheY reduces binding to CheA but enhances binding to CheZ and FliM. Measurement of the binding affinities between CheY D13K and each of these three proteins may therefore indicate the degree of structural similarity between CheY D13K and CheY-P. D13K binds to CheA with about 2-fold lower affinity than nonphosphorylated wild-type CheY (46, 51), but its binding affinities for CheZ (47) and FliM (34) are the same as nonphosphorylated wild-type rather than the enhanced affinities expected for an activated conformation of CheY-P. Thus, the *in vitro* protein binding assays suggest that CheY D13K only partially assumes the activated conformation in solution.

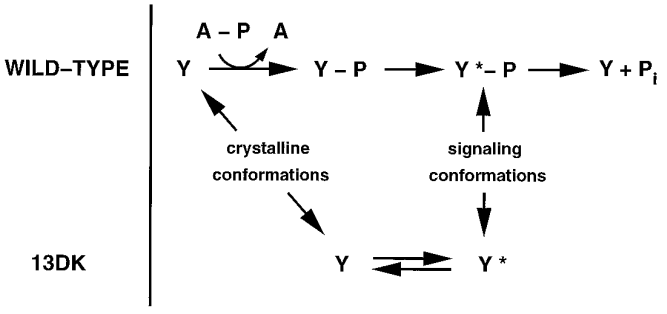

FIG. 5. **Schematic diagram of possible activation pathways for wild-type CheY and CheY D13K.**

Several other observations support the hypothesis that CheY D13K exists in a metastable state, in a conformation that can easily convert to the activated form. First, the hyper-signaling activity of CheY D13K is observed in a strain containing a multicopy plasmid (25) but is substantially reduced when the mutant protein is expressed from a single copy chromosomal gene (26). Second, the *in vivo* activity of wild-type CheY is increased by simple overexpression (52), and there is evidence that nonphosphorylated wild-type CheY possesses a low level of clockwise-generating activity (10). Finally, in the case of

[2] D. Lowry and F. W. Dahlquist, unpublished observations.

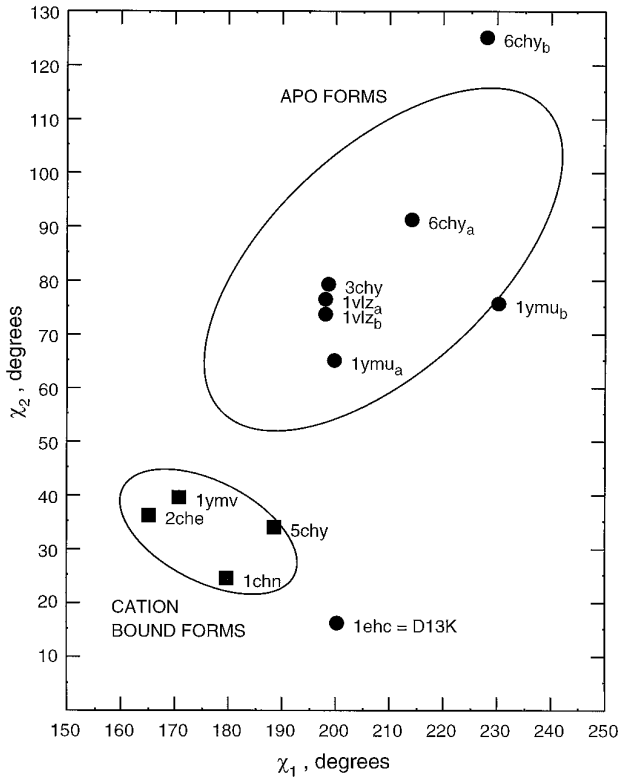

FIG. 6. **Plot of χ_1 *versus* χ_2 angles for the aspartate 57 residue of wild-type CheY and all known mutant structures.** The average values of χ_1 and χ_2 are 208° and 84°, respectively, for the apo forms (●), excluding D13K, and 177° and 33°, respectively, for the cation bound forms (■). The *ellipses* enclose a range of four standard deviations for the two populations. The conformation in D13K is closer to the cation bound structures and is away from the apo forms. The conformation of aspartate 57 is shown in Fig. 4*A* for wild-type and in Fig. 4*B* for D13K. The apo structures are wild-type (*3chy*; Ref. 14); T87I (*1vlz*, 2 molecules; Ref. 23); M17G (*1ymu*, 2 molecules; Ref. 54); T87I/Y106W (*6chy*, 2 molecules; Ref. 56); and D13K (*1ehc*, this work). The cation bound structures are wild-type CheY:Mg^{2+} (*2che*; Ref. 15; and *1chn*; Ref. 16); F14G/S15G/M16G:Mg^{2+} (*1ymv*; Ref. 54); and Y106W:Ca^{2+} (*5chy*; Ref. 56).

another response regulator, OmpR, overproduction of the non-phosphorylatable mutant D55Q (position 55 being the site of phosphorylation of OmpR) generates the phenotype characteristic of wild-type OmpR-P (53).

^{19}F-NMR Results Regarding the Conformational State of CheY D13K—The CheY molecule contains six phenylalanine residues. Four of these (Phe^8, Phe^{30}, Phe^{53}, and Phe^{124}) are clustered far from the active site, Phe^{14} is solvent exposed, and Phe^{111} is buried underneath Lys^{109}. ^{19}F-NMR spectra obtained with 4-fluorophenylalanine-labeled CheY D13K did not show any differences in the environments of Phe^8, Phe^{30}, Phe^{53}, and Phe^{124} between wild-type CheY and CheY D13K (26), suggesting that the D13K substitution does not induce a conformational change in this remote region. This is consistent with the conformation observed in the CheY D13K crystal structure. The resonance for 4-fluorophenylalanine-labeled Phe^{111} was perturbed, perhaps reflecting an effect of the D13K substitution on the position of Lys^{109}. However, the environment of Phe^{111} is essentially identical in the crystal structures of wild-type CheY and CheY D13K. The only structural differences in the crystallographic results involve the two aspartate residues, Asp^{12} and Asp^{57}, discussed above, which are more than 7 Å away from Phe^{111}. Thus, the ^{19}F-NMR work also suggests that CheY D13K adopts a conformation in solution different than that observed in the crystal structure presented here.

Conclusions and Possible Mechanisms for CheY D13K Activation—In summary, the crystal structure of the constitutively active D13K mutant of CheY surprisingly has no conformational differences when compared with the Mg^{2+}-free form of the wild-type CheY molecule. Thus the CheY D13K structure presented here is the inactive form of the molecule, and the interpretation is that only in solution does this form proceed to a conformation resembling activated CheY.

In all CheY structures published to date, (14–16, 23, 54, 56), the Asp^{57} side chain assumes one of two general positions, depending upon the presence or absence of a divalent cation (Mg^{2+} or Ca^{2+}) (Fig. 6). In the apo forms, Asp^{57} and Lys^{109} have strong bonding interactions, but introduction of Mg^{2+} or Ca^{2+} eliminates this interaction (15, 16, 54, 56). Phosphorylation of Asp^{57} is certain to rearrange the active site even further, requiring a repositioning of the Lys^{109} side chain (14). Lys^{109} is known to be essential for stimulation of clockwise flagellar rotation but not for phosphorylation or autodephosphorylation of CheY (24, 26), and thus, it has a presumed role in the propagation of a conformational change that causes activation. The unusual position of the Asp^{57} side chain in CheY D13K may reflect a predisposition of this mutant form of CheY to readily assume the activated conformation in the absence of phosphorylation.

An alternate activation mechanism is that CheY D13K might mimic a part of the CheY-P structure that is important for clockwise signal generation but lacks the conformation needed for efficient FliM binding since CheY D13K does not exhibit the enhanced binding to FliM *in vitro* observed with wild-type CheY-P (34). The fact that we found D13K in an "inactive" conformation is consistent with this, again suggesting that the activity resides in only a minor sub-population of the molecules. Thus it is possible that FliM binding and promotion of clockwise flagellar rotation may be separable events. It has been proposed elsewhere (10, 34, 55) that binding of CheY-P to the flagellar motor is a necessary, but not sufficient, event for signal transduction.

Acknowledgments—We thank E. Westbrook and M. Westbrook for help and generosity in data collection at Argonne National Laboratory.

REFERENCES

1. Parkinson, J. S., and Kofoid, E. C. (1992) *Annu. Rev. Genet.* **26,** 71–112
2. Parkinson, J. S. (1993) *Cell* **73,** 857–871
3. Swanson, R. V., Alex, L. A., and Simon, M. I. (1994) *Trends Biochem. Sci.* **19,** 485–490
4. Hoch, J. A., and Silhavy, T. J. (1995) *Two-Component Signal Transduction*, ASM Press, Washington, D. C.
5. Lukat, G. S., McCleary, W. R., Stock, A. M., and Stock, J. B. (1992) *Proc. Natl. Acad. Sci. U. S. A.* **89,** 718–722
6. McCleary, W. R., and Stock, J. B. (1994) *J. Biol. Chem.* **269,** 31567–31572
7. Larsen, S. H., Reader, R. W., Kort, E. N., Tso, W.-W., and Adler, J. (1974) *Nature* **249,** 74–77
8. Wylie, D., Stock, A., Wong, C.-Y., and Stock, J. (1988) *Biochem. Biophys. Res. Commun.* **151,** 891–896
9. Hess, J. F., Oosawa, K., Kaplan, N., and Simon, M. I. (1988) *Cell* **53,** 79–87
10. Barak, R., and Eisenbach, M. (1992) *Biochemistry* **31,** 1821–1826
11. Berg, H. C., and Brown, D. A. (1972) *Nature* **239,** 500–504
12. Macnab, R. M., and Koshland, D. E., Jr. (1972) *Proc. Natl. Acad. Sci. U. S. A.* **69,** 2509–2512
13. Stock, A. M., Mottonen, J. M., Stock, J. B., and Schutt, C. E. (1989) *Nature* **337,** 745–749
14. Volz, K., and Matsumura, P. (1991) *J. Biol. Chem.* **266,** 15511–15519
15. Stock, A. M., Martinez-Hackert, E., Rasmussen, B. F., West, A. H., Stock, J. B., Ringe, D., and Petsko, G. A. (1993) *Biochemistry* **32,** 13375–13380
16. Bellsolell, L., Prieto, J., Serrano, L., and Coll, M. (1994) *J. Mol. Biol.* **238,** 489–495
17. Bruix, M., Pascual, J., Santoro, J., Prieto, J., Serrano, L., and Rico, M. (1993) *Eur. J. Biochem.* **215,** 573–585
18. Moy, F. J., Lowry, D. F., Matsumura, P., Dahlquist, F. W., Krywko, J. E., and Domaille, P. J. (1994) *Biochemistry* **33,** 10731–10742
19. Santoro, J., Bruix, M., Pascual, J., Lopez, E., Serrano, L., and Rico, M. (1995) *J. Mol. Biol.* **247,** 717–725
20. Volz, K. (1993) *Biochemistry* **32,** 11741–11753
21. Lukat, G. S., Stock, A. M, and Stock, J. B. (1990) *Biochemistry* **29,** 5436–5442
22. Sanders, D. A., Gillece-Castro, B. L., Stock, A. M., Burlingame, A. L., and Koshland, D. E., Jr. (1989) *J. Biol. Chem.* **264,** 21770–21778
23. Ganguli, S., Wang, H., Matsumura, P., and Volz, K. (1995) *J. Biol. Chem.* **270,** 17386–17393

24. Lukat, G. S., Lee, B. H., Mottonen, J. M., Stock, A. M., and Stock, J. B. (1991) *J. Biol. Chem.* **266,** 8348–8354
25. Bourret, R. B., Hess, J. F., and Simon, M. I. (1990) *Proc. Natl. Acad. Sci. U. S. A.* **87,** 41–45
26. Bourret, R. B., Drake, S. K., Chervitz, S. A., Simon, M. I., and Falke, J. J. (1993) *J. Biol. Chem.* **268,** 13089–13096
27. Roman, S. J., Meyers, M., Volz, K., and Matsumura, P. (1992) *J. Bacteriol.* **174,** 6247–6255
28. Drake, S. K., Bourret, R. B., Luck, L. A., Simon, M. I., and Falke, J. J. (1993) *J. Biol. Chem.* **268,** 13081–13088
29. Lowry, D. F., Roth, A. F., Rupert, P. B., Dahlquist, F. W., Moy, F. J., Domaille, P. J., and Matsumura, P. (1994) *J. Biol. Chem.* **269,** 26358–26362
30. Hess, J. F., Bourret, R. B., and Simon, M. I. (1991) *Methods Enzymol.* **200,** 188–204
31. Koeppe, R. E., II, Stroud, R. M., Pena, V. A., and Santi, D. V. (1975) *J. Mol. Biol.* **98,** 155–160
32. Volz, K., Beman, J., and Matsumura, P. (1986) *J. Biol. Chem.* **261,** 4723–4725
33. Hess, J. F., Bourret, R. B., Oosawa, K., Matsumura, P., and Simon, M. I. (1988) *Cold Spring Harbor Symp. Quant. Biol.* **53,** 41–48
34. Welch, M., Oosawa, K., Aizawa, S.-I., and Eisenbach, M. (1994) *Biochemistry* **33,** 10470–10476
35. Howard, A., Gilliland, G. L., Finzel, B. C., Poulos, T. L., Ohlendorf, D. H., and Salemme, F. R. (1987) *J. Appl. Crystallogr.* **20,** 383–390
36. Hendrickson, W. A. (1985) *Methods Enzymol.* **115,** 252–270
37. Hall, S. R., and Stewart, J. M. (eds) (1988) *XTAL 2.4 User's Manual*, Universities of Western Australia and Maryland, Perth, Australia
38. Finzel, B. F. (1987) *J. Appl. Crystallogr.* **20,** 53–55
39. Jones, T. A. (1985) *Methods Enzymol.* **115,** 157–171
40. Hurley, J. H., Dean, A. M., Thorsness, P. E., Koshland, D. E., Jr., and Stroud, R. M. (1990) *J. Biol. Chem.* **265,** 3599–3602
41. Hurley, J. H., Dean, A. M., Sohl, J. L., Koshland, D. E., Jr., and Stroud, R. M. (1990) *Science* **249,** 1012–1016
42. Kar, L., Matsumura, P., and Johnson, M. E. (1992) *Biochem. J.* **287,** 521–531
43. McNally, D. F., and Matsumura, P. (1991) *Proc. Natl. Acad. Sci. U. S. A.* **88,** 6269–6273
44. Schuster, S. C., Swanson, R. V., Alex, L. A., Bourret, R. B., and Simon, M. I. (1993) *Nature* **365,** 343–347
45. Swanson, R. V., Schuster, S. C., and Simon, M. I. (1993) *Biochemistry* **32,** 7623–7629
46. Li, J., Swanson, R. V., Simon, M. I., and Weis, R. M. (1995) *Biochemistry* **34,** 14626–14636
47. Blat, Y., and Eisenbach, M. (1994) *Biochemistry* **33,** 902–906
48. Blat, Y., and Eisenbach, M. (1996) *J. Biol. Chem.* **271,** 1226–1231
49. Blat, Y., and Eisenbach, M. (1996) *J. Biol. Chem.* **271,** 1232–1236
50. Welch, M., Oosawa, K., Aizawa, S.-I., and Eisenbach, M. (1993) *Proc. Natl. Acad. Sci. U. S. A.* **90,** 8787–8791
51. Shukla, D., and Matsumura, P. (1995) *J. Biol. Chem.* **270,** 24414–24419
52. Clegg, D. O., and Koshland, D. E., Jr. (1984) *Proc. Natl. Acad. Sci. U. S. A.* **81,** 5056–5060
53. Kanamaru, K., and Mizuno, T. (1992) *J. Biochem.* **111,** 425–430
54. Bellsolell, L., Cronet, P., Majolero, M., Serrano, L., and Coll, M. (1996) *J. Mol. Biol.* **257,** 116–128
55. Zhu, X. Y., Amsler, C. A., Volz, K., and Matsumura, P. (1996) *J. Bacteriol.* **178,** 4208–4215
56. Zhu, X. Y., Rebello, J., Matsumura, P., and Volz, K. (1997) *J. Biol. Chem.* **272,** 5000–5006